

7th Asian-Pacific Conference on Aerospace Technology and Science, 7th APCATS 2013

Study on Judgment Method of Combustion Mode on dual-mode Scramjet

Q. Chen^a, L. H. Chen^a, H. B. Gu^a, X. Y. Zhang^a, P. Wang^{b,*}

^aState Key Laboratory of High-Temperature Gas Dynamics, Institute of mechanics, Chinese academy of sciences, Beijing, 100190, China

^bChina University of Petroleum, Beijing, 102249, China

Abstract

It was very significant to judge the combustion mode of engine correctly, because the distributions of fuels and other parameters of combustion mode switching depended on it. This paper proposed to a judgment method of combustion mode of engine, namely artificial neural network method, based on the dual-mode scramjet experiments and analysis results. It made use of experimental measurement values, and the parameters along engine were obtained through one dimensional analysis. This method provided the basis for the combustion mode design of engine in the future.

© 2013 The Authors. Published by Elsevier Ltd.

Selection and peer-review under responsibility of the National Chiao Tung University

Keywords: Combustion mode, Scramjet, Artificial neural network

Nomenclature

A	area
C_f	skin friction coefficient
C_{fuel}	coefficient of fuel distribution
c_p	specific heat at constant pressure
h	specific enthalpy
M	Mach number
p	static pressure
R_{Ac}	area ratio of combustor outlet to inlet
T	static temperature

* Corresponding author. Tel.: +86-10-89731770.

E-mail address: wangpei@amss.ac.cn

V	velocity
$X_{H_2O, vit}$	mole fraction of water vapor in the vitiator products
x	position in x-direction
Y	mass fraction
<i>Greek symbols</i>	
γ	ratio of specific heat
η	combustion efficiency
η_{sto}	stoichiometric combustion efficiency
ρ	density
ϕ	stoichiometric ratio
<i>Subscripts</i>	
i	component

1. Introduction

In the range of flight altitude 18~30 km and flight Mach number 4~7, the dual-mode scramjet with hydrocarbon fuels is one of the most competitive air breathing propulsion systems [1, 2]. In order to maintain the high performance of engine in the range of flight altitude and Mach number, the combustion mode in combustor is necessary to be switched [3]. In general, at lower flight altitude and Mach number, an engine with subsonic combustion mode attains higher performance than an engine with supersonic combustion mode. On the contrary, a supersonic combustion mode engine has the higher performance at higher altitude and Mach number. It was very significant to judge the combustion mode of engine correctly, because the distributions of fuels and other parameters of next combustion mode switching depended on it.

With the drastic development of computer technology, the artificial neural network method had made great applications in many fields, such as high performance aircraft autopilots, flight path simulations, aircraft component fault detectors [4]. One of the most important applications was pattern recognition technology. A neural network was able to learn to recognize the pattern from the observed data or experiment data. That was a novel method to judge the combustion mode of dual-mode Scramjet engine.

Based on the dual-mode scramjet experiments and analysis results, this article proposed to a judgment method of combustion mode of engine, namely artificial neural network method. It made use of experimental measurement values, such as burned and unburned pressure distributions, fuel injection positions, and fuel equivalence ratios. The parameters along engine were obtained through one dimensional analysis. Then they were treated as learning cases of the neural network. After being trained by the learning cases, the judgment model was established, providing the basis for the combustion mode design of engine in the future.

2. Experimental Setup and Analysis Method

2.1. Experimental Setup

The experiments applied to the paper were performed on the direct-connected facility which was specially designed for dual-mode scramjet combustor experiments. The experimental gas was heated by a vitiator, which burned hydrogen and replenished oxygen to maintain oxygen mole percentage at 21% in the experimental gas. There were two types of condition at the entrance of isolator. The details of the flow parameters were shown in

Table 1.

Table 1 Operation parameters of facility

Mach number	Total temperature(K)	Total pressure (MPa)	Mass ratio(kg/s)
1.8	950	0.6	1.8
2.5	1650	1.0	1.2

There were also three types of test models, which were named as Model-1, Model-2, and Model-3 to perform experiments. The schematics of the test models were shown in Fig.1. The test model consisted of isolator, combustor and nozzle. Three models had the same isolator. The differences of the models were the expansion angles of the combustor. The combustor of Model-1 had three expansion sections with angles of 1.5°, 2.0° and 3°. However, Model-2 and Model-3 only had two expansion sections and the angles were 1.5°, 2° and 1.5°, 3° respectively. The fuel C₂H₄ was injected into and burned in a cavity-based flame holder. The positions of fuel jet were shown in Fig.1.

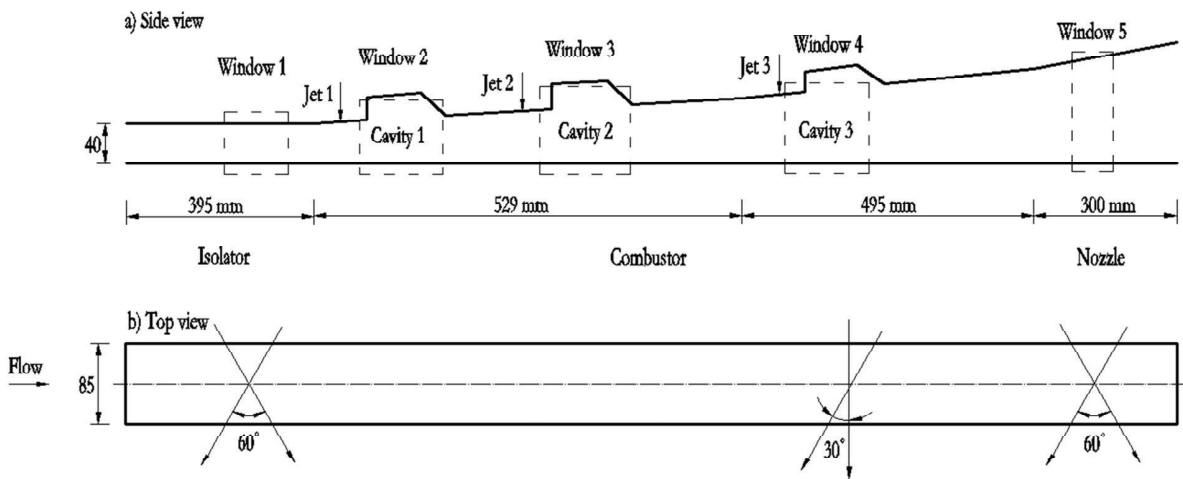


Fig.1 Schematic of direct-connected scramjet test facility

2.2. Quasi 1-D Analytical Method

In order to analyze the experimental data deeply, this paper developed a quasi-1-D analytical model based on the experimental data. One step chemical reaction was assumed that includes only the major species of C₂H₄, H₂O, CO₂, O₂, and N₂. The chemical equation was shown in Equ.(1) where ϕ and η respectively represented stoichiometric ratio and combustion efficiency. $X_{H_2O,vit}$ was the mole fraction of water vapor in the vitiator products.

$$\phi C_2H_4 + 3 \left(O_2 + \frac{X_{H_2O,vit}}{0.21} H_2O + \left(3.76 - \frac{X_{H_2O,vit}}{0.21} \right) N_2 \right) = (1-\eta) \phi C_2H_4 + 3(1-\phi\eta) O_2 + \left(2\phi\eta + 3 \frac{X_{H_2O,vit}}{0.21} \right) H_2O + 2\phi\eta CO_2 + 3 \left(3.76 - \frac{X_{H_2O,vit}}{0.21} \right) N_2 \tag{1}$$

Equ.(2)~(5) were the governing equations of the analytical method. They were mass, momentum, energy conservation equations and state equation. Assuming that the combustor wall was adiabatic, the term of convective heat transfer did not exist in Equ.(3).

$$\frac{d\rho}{dx} = -\frac{\rho}{V} \frac{dV}{dx} - \frac{\rho}{A} \frac{dA}{dx} \quad (2)$$

$$\frac{dV}{dx} = -\frac{V}{\gamma M^2} \left(\frac{1}{p} \frac{dp}{dx} + 2 \frac{\gamma M^2 C_f}{D} \right) \quad (3)$$

$$\frac{dT}{dx} = -\frac{1}{c_p} \left(\sum_i h_i \frac{dY_i}{dx} + V \frac{dV}{dx} \right) \quad (4)$$

$$\frac{1}{\rho} \frac{d\rho}{dx} + \frac{1}{T} \frac{dT}{dx} - \frac{1}{p} \frac{dp}{dx} = 0 \quad (5)$$

The skin friction coefficient C_f in Equ.(3) was determined using the method given by JAXA [5] where:

$$C_f = \frac{0.38 \left(1 + \frac{\gamma-1}{2} M^2 \right)^{-0.467}}{(\log \text{Re}_x)^{2.58}} \quad (6)$$

For the governing equations, a continuous wall pressure distribution $p(x)$ was needed to solve the equations system. This distribution function could be obtained from the discrete experimental data by creating 3-peak Gaussian fits. The Gaussian peaks were encountered in many areas of science and engineering, and was given by

$$p = \sum_{i=1}^3 a_i \exp \left[-\left(\frac{x-b_i}{c_i} \right)^2 \right]$$

Where a , b , c were respectively the amplitude, the centroid (location) and the peak width. The engineering enthalpy of each species was a function of the temperature ($h_i(T)$) [6]. These values were obtained at a given temperature from the tabulated thermodynamic data in the Burcat's report. Y_i was the mass fraction of species i , and the term dY_i/dx could be written as the function of $d\eta/dx$. Because the mole quantities did not change during the processing of C_2H_4 combustion, the average molecular weight did not change. So, the state equation could be written as Equ.(5).

In the system of equations, there were nine unknown variables which were ρ, V, T, η, Y_i . And there were also nine differential equations including four equations of dY_i/dx and $d\eta/dx$. So, the equations system could be integrated through the numerical method.

2.3. Radial Basis Function (RBF) neural network

RBF neural network (Fig.2) was a feed forward network with three layers based on regularization theory. A Gaussian RBF monotonically decreased with distance from the center (Fig.2(b)). So, Gaussian-like RBFs were local (give a significant response only in a neighborhood near the response only in a neighborhood near the center) and are more commonly used than multiquadric-type RBFs which have a global response. They are also more biologically plausible because their response is finite.

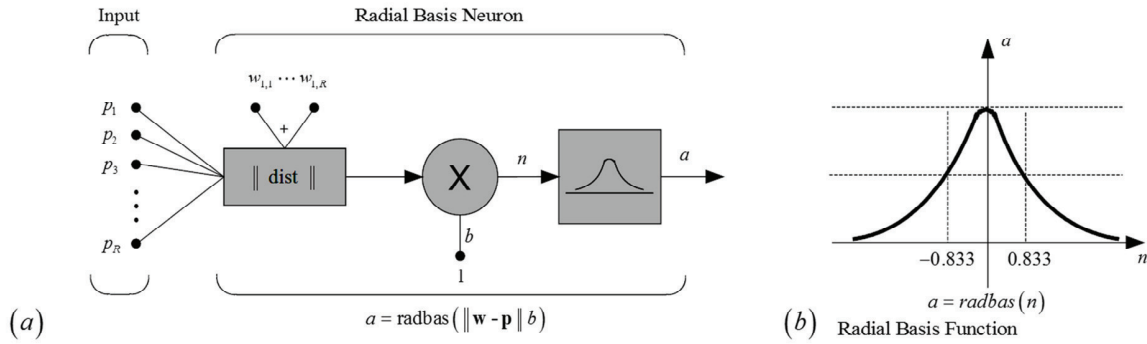


Fig.2 Architecture of RBF neural networks, (a) Radial basis neuron, (b) Radial basis function

At present, the RBF Neural network can deal well with the problem including classification and pattern discrimination. The problem of Scramjet combustion modes diagnose belonged to the category. RBF Neural network required a supervised learning the existing classification results, then the network would update the weights of neurons. After the learning processing was completed, the network would be able to classify the new inputs.

In this paper, considering the characteristics of scramjet combustion parameters, the inputs of RBF network in this problem were listed in Table 2. R_{Ac} represented the extend of combustor expansion, C_{fuel} represented the conditions of fuel distribution, and the bigger the value was, the distribution of fuel was near to the combustor outlet. η_{sto} represented the relative quantities of heat release.

Table 2 Inputs of RBF network

Input	Expression	Range of input	Clarification
$M_{iso,in}$	-	1.8, 2.5	Mach number at outlet of isolator
R_{Ac}	$A_{combustor,out} / A_{combustor,in}$	1.8525, 1.895, 1.9825	Area ratio of combustor outlet to inlet
C_{fuel}	$\sum (\phi_i / \phi) \cdot (x_{fuel_jet_i} / L_{combustor})$	0.55–0.86	Coefficient of fuel distribution
η_{sto}	$\eta \cdot \phi$	0.12–0.55	Stoichiometric combustion efficiency

3. Results and Discussion

3.1. Analysis of the experimental results

There had been 30 experiments with different conditions for three types of engine models, which were carried out at the direct-connected scramjet test facility. Among the experiments, there were 14 times of experiments whose condition of the entrance was Mach number 1.8, and other experiments were Mach number 2.5. The fuel equivalence ratio was between 0.3 and 0.8 at these experiments. In Fig.3, two typical experimental parameters distributions were shown. The blue dots showed in the illustrations represented the experimental pressure distributions along the combustor. The black lines at the bottom of the figure depicted the inner passage of the combustor. The Mach number at the entrance was 2.5 in Fig.3(a), 1.5 in Fig.3(b). And the other detailed flow parameters at entrance were shown in Table 2 and Table 3. In experiment (a) the fuel C_2H_4 was injected into the combustor at two different positions and the total equivalent ratio was 0.38. In experiment (b), the fuel C_2H_4 was

injected into the combustor at 4 positions and the equivalent ratio was 0.56. At the aspect of the distribution parameter of fuel C_{fuel} , the fuel layout of the experiment (a) was front of experiment (b) relatively.

Applying the quasi-one-dimensional analytical method mentioned in section 2.1, the distributions of parameters could be obtained in the combustor. The distributions of Mach number (green lines), static pressure P (blue lines), and combustion efficiency (red lines) were shown in Fig.3. The figure showed that the trend of static pressure distribution measured by experiments was well fitted through the method of Gaussian fitting. Experiment (a) was at supersonic combustion mode, because the Mach number was greater than 1 in the combustor. However, for experiment (b), Mach number was under 1 in some region, though the flow returned to supersonic flow at back of combustor. So, experiment (b) would be judged as the subsonic combustion mode. At the aspect of combustion efficiency, the combustion of supersonic mode was relatively severer than subsonic mode, because combustion efficiency curve of supersonic mode rose rapidly at the shorter region. However, the efficiency curve of subsonic combustion mode was more uniform in combustor.

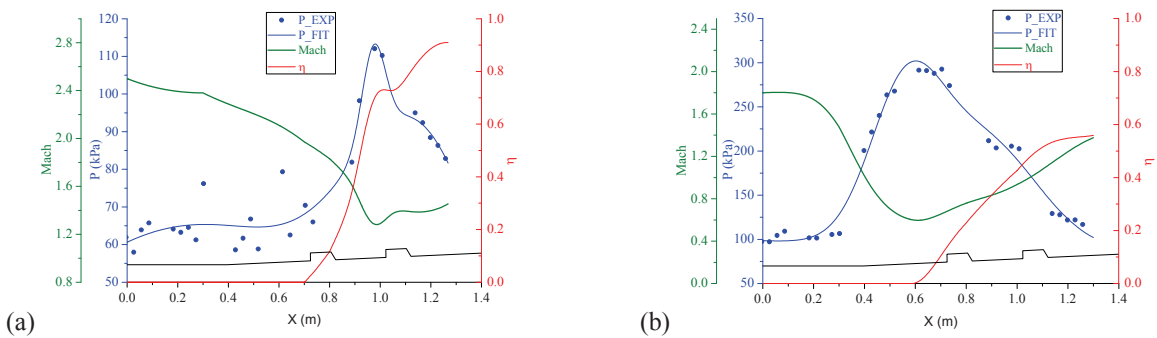


Fig.3 Distributions of flow parameters in the combustor for (a) supersonic combustion mode and (b) subsonic combustion mode

Table 3 Parameters of experiment (a) and (b)

Input	(a)	(b)
$M_{iso,in}$	2.5	1.8
R_{Ac}	1.982	1.895
C_{fuel}	0.77	0.81
η_{sto}	0.35	0.32

3.2. RBF neural network modeling

Depending on Mach number distribution along the engine, the combustion mode of the experiment could be judged. For 30 experiments under different working conditions, the distributions of Mach number could be obtained through the method introduced in section 2.1. Then the RBF neural network model for combustion mode determining could be established according to the method from section 2.2. The RBF neural network's inputs contained four groups of parameters were shown in Table 2.

In order to verify the robustness of the network, the 25 samples were randomly selected from 30 experiments as the training set. And the five rest samples (two experiments of supersonic combustion mode and three experiments of subsonic combustion mode) were used as the test set, to verify the judgment ability of the network.

The neural network of mode determining was consisted of 25 neurons and divided into two layers. By learning from samples, the neuron weight matrix was updated. For the five test samples, the network had predicted the combustion mode rightly. Namely, the RBF neural network had good adaptability to the problems of combustion mode classification.

3.3. The parameters analysis of engine combustion mode

The parameter analysis of combustion mode was carried out in this paper through RBF neural network model. The supercritical curve of supersonic/subsonic combustion mode was obtained when some parameters were fixed. Fig.4 showed the combined effects of the coefficient of fuel distribution C_{fuel} and stoichiometric combustion efficiency η_{sto} on combustion mode when $M_{iso in}$ and R_{Ac} were fixed.

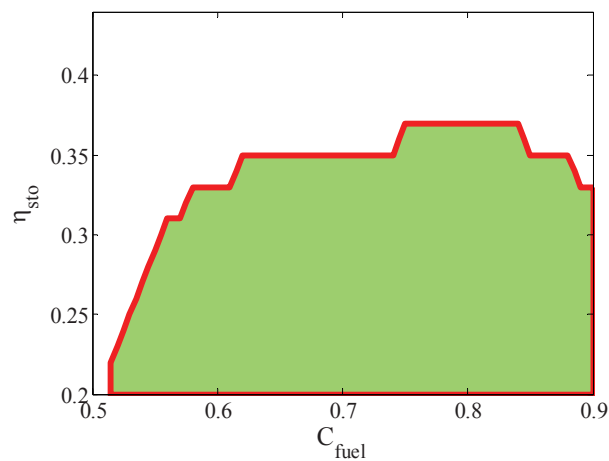


Fig.4 Effects of C_{fuel} and η_{sto} on the combustion mode

Fig.4 showed when the situations were in the green range, the scramjet was at supersonic combustion mode. But in other regions the scramjet was at subsonic combustion or unstarted mode. It also could be known when C_{fuel} is smaller than 0.65 (fuel was mainly injected at the forward section of combustor), the engine mode was affected by the combined influences of C_{fuel} and η_{sto} . The engine could not maintain the supersonic mode unless the fuel mainly released heat at the back of the combustor when η_{sto} rose. When C_{fuel} was greater than 0.65, the relationship between mode and fuel distribution coefficient of the engine was no longer significant. In addition, when η_{sto} was greater than 0.35, the engine could not maintain supersonic mode no matter how the fuel distribution in the combustor. The engine would turn into the subsonic or unstarted mode.

4. Conclusions

In this paper the combustion mode of dual-mode scramjet judgment method was developed. Direct-connected experimental results of three scramjet combustor models and two entrance situations were analyzed by a one-dimensional method. The important parameters were obtained, such as C_{fuel} , η_{sto} and the combustion mode. Then the judgment model based on the RBF neural network was built by learning the obtained combustion mode. The followings were the conclusions:

(1) One-dimensional analysis method was able to calculate the flow parameters of the engine combustor effectively.

(2) RBF neural network models could be applied to judge the engine combustion mode, and the accuracy of judgment was acceptable.

(3) Under the inner geometry and entrance conditions unchanged, the combustion mode was affected by C_{fuel} and η_{sto} when η_{sto} was relatively small. However, when η_{sto} was larger, the combustion mode was less affected by C_{fuel} .

Acknowledgements

The project is partially supported by the State Key Laboratory of High-Temperature Gas Dynamics Foundation and China University of Petroleum Foundation (KYJJ2012-06-07)

References

- [1] E. T. Curran, F. D. Stull, 1964. "The utilization of supersonic combustion ramjet systems at low mach numbers", Aero Propulsion Laboratory, RTD-TDR-63-4097.
- [2] F. Billig, 1988. Combustion processes in supersonic flow, Journal of Propulsion and Power, 4(3), 209-216.
- [3] S. Tomioka, K. Tani, R. Masumoto, S. Ueda, 2009. "Dual-mode operation of a rocket-ramjet combined cycle engine", 27th International Symposium on Space Technology and Science, Tsukuba (Japan), ISTS Paper 2009-a-26.
- [4] Hagan, Martin T., Howard B. Demuth, and Mark H. Beale, 1996. Neural Network Design, 1st ed. 1 vols Boston: PWS Pub.
- [5] Mitani, T., Hiraiwa, T., Tarukawa, et al, 2002. Drag and total pressure distributions in scramjet engines at Mach 8 flight, Journal of Propulsion and Power, 18(4): p. 953-960.
- [6] Alexander Burcat and Branko Ruscic, 2005. "Third Millennium Ideal Gas and Condensed Phase Thermochemical Database for Combustion with Updates from Active Thermochemical Tables", Argonne National Laboratory Report, ANL-05/20 TAE 960.